PAPER

Defects-assisted piezoelectric response in liquid exfoliated MoS_2 nanosheets

To cite this article: Jyoti Shakya *et al* 2022 *Nanotechnology* **33** 075710

IOP Publishing Nanotechnology
Nanotechnology 33 (2022) 075710 (7pp) https://doi.org/10.1088/1361-6528/ac368b

Defects-assisted piezoelectric response in liquid exfoliated MoS_2 nanosheets

Jyoti Shakya[1,*], **Gayathri H N**[1] and **Arindam Ghosh**[1,2]

[1] Department of Physics, Indian Institute of Science, Bangalore 560012, India
[2] Centre for Nano Science and Engineering, Indian Institute of Science, Bangalore 560012, India

E-mail: jyiitd@gmail.com

Received 12 September 2021, revised 28 October 2021
Accepted for publication 4 November 2021
Published 26 November 2021

Abstract

MoS_2 is an intrinsic piezoelectric material which offers applications such as energy harvesting, sensors, actuators, flexible electronics, energy storage and more. Surprisingly, there are not any suitable, yet economical methods that can produce quality nanosheets of MoS_2 in large quantities, hence limiting the possibility of commercialisation of its applications. Here, we demonstrate controlled synthesis of highly crystalline MoS_2 nanosheets via liquid phase exfoliation of bulk MoS_2, following which we report piezoelectric response from the exfoliated nanosheets. The method of piezo force microscopy was employed to explore the piezo response in mono, bi, tri and multilayers of MoS_2 nanosheets. The effective piezoelectric coefficient of MoS_2 varies from 9.6 to 25.14 pm V^{-1}. We attribute piezoelectric response in MoS_2 nanosheets to the defects formed in it during the synthesis procedure. The presence of defects is confirmed by x-ray photoelectron spectroscopy.

Keywords: 2D materials, MoS_2, piezoelectricity

(Some figures may appear in colour only in the online journal)

1. Introduction

Piezoelectricity is the charge that originated when certain materials are placed under stress. The stretching or compressing of the substance induces electricity and allows the facile turning of mechanical energy into electrical and vice versa which offers an immense application for sensors, energy harvesting, flexible electronics, energy storage, and actuators. A great deal of research is being carried out in generating clean energy due to obvious reasons [1, 2]. It is very essential to find sustainable and environment friendly non-conventional forms of energy. To substitute conventional fuels, one way is to harvest electricity from human surroundings. The piezoelectric systems could prove extremely useful in such a scenario. Piezoelectricity at micro and nanoscale can be effectively engineered by necessary surface modifications including the introduction of adatoms and defects in such materials leading to surface piezoelectricity. Vast amount of research has been reported on piezoelectricity in various inorganic and organic based materials including composites [3–5]. However, the above-mentioned piezoelectric materials have some drawbacks due to their lower piezoelectric properties, non-biodegradability, rigidity, toxic nature, non-ecofriendliness, and non-biocompatibility. In search of efficient piezoelectric material, 2D materials are emerging as a potential alternative as theoretically predicted and some of them have been confirmed experimentally [6–8]. The transition metal dichalcogenides (TMDCs) in particular have been explored increasingly due to their non-centrosymmetric crystal structure and large surface area to thickness ratio [9–11]. As a typical TMDC material, MoS_2 is of great interest due to its novel properties such as tunable band gap, large in-plane mobility, and mechanical stability [12–15]. Each layer of MoS_2 is made up of Mo atoms sandwiched between two layers of hexagonally close-packed S atoms, and the weak van der Waals forces tie the sandwiched adjacent layers [16]. Ultrathin MoS_2 layers can be prepared through various techniques such as hydrothermal method, liquid phase exfoliation (LPE), chemical vapor deposition, mechanical exfoliation, and so on [17–20]. Among these techniques, LPE method looks promising for scalable production of MoS_2 because of its low cost,

* Author to whom any correspondence should be addressed.

relatively high output and simplicity. But controlled synthesis of crystalline MoS_2 with desired structure and morphology is still a challenge.

In case of MoS_2 it has been observed that the odd layered MoS_2 is highly piezoelectric due to non-centrosymmetric nature, with monolayer showing the strong piezoelectricity [9, 21]. The piezoelectric effect disappears in bulk MoS_2 due to the opposite orientations of the adjacent layers. Most of these demonstrations of piezoelectric effect have been made on mechanically exfoliated odd number of nanosheets which pose limitations for large scale applications. As an alternative, the technique of LPE along with fabrication techniques like solution casting, spray coating, or inkjet printing can be used for scalable fabrication of electronic devices. In this direction, some theoretical research on piezoresponse in multilayer 2D materials has been reported but intensive experimental studies are still lacking [9, 11, 22]. To the best of our knowledge, no experimental report is available on the piezoelectric response from the liquid phase exfoliated few layers of MoS_2. In this work, we propose that 2D MoS_2 layers synthesized via modified LPE method contain defects that can act as prime spots for trapping charges and display piezo signals.

2. Experimental details

The MoS_2 nanosheets were prepared by modified LPE method. In detail, 2g of MoS_2 powder (<6 μm, 98%, Sigma) was dispersed in 60 ml water and probe sonicated for 1 h to get a homogeneous mixture. The obtained mixture was kept in a hydrothermal autoclave reactor and subjected to continuous stirring for 3 h at 150 °C. The pre-treated MoS_2 was diluted in IPA/water and further exfoliated using a probe sonicator for about 5 h. The obtained dispersion was centrifuged at 5000 rpm for 30 min to collect the supernatant. The collected supernatant was further diluted before coating on a substrate to avoid nanosheet agglomeration. Few trials of the spin coating were made to get un-agglomerated coating of nanosheets on ITO substrate for all PFM measurements.

3. Characterization

The surface morphology of MoS_2 nanosheets was observed and analyzed by scanning electron microscope coupled with energy dispersive x-ray (SEM-EDX) spectroscopy (Ultra55 FE-SEM Karl Zeiss). All the SEM images were taken under the operating voltage of 5 kV in InLens mode. The qualitative analysis was performed using energy dispersing x-ray spectroscopy (EDS) at electron high tension voltage of 15 kV. The Raman spectra were taken at room temperature using Horiba LabRAM HR Raman spectrometer. Instrument resolution was ~0.5 cm^{-1} by using 1800 groove mm^{-1} grating. A linearly polarized laser light (532 nm) was used for the measurements keeping the laser power below 1 mW. Structural analysis and mapping were carried out using a transmission electron microscope (TEM TITEN Themis) conducted at accelerating voltage of 200 kV. For TEM analysis, diluted MoS_2 dispersion was drop cast over a carbon-coated copper grid, followed by drying under IR bulb. The PFM measurements were carried out using an atomic force microscope (AFM), Park system (Park AFM NX 20). A conducting cantilever (Multi75E-G) having a force constant of 3 N m^{-1} and resonant frequency 75 kHz was employed in all our PFM measurements.

4. Results and discussion

The morphology of MoS_2 layers was characterized by TEM as shown in figure 1(a), which suggests the presence of very thin sheets. A clear view of lattice fringes having the lattice spacing of the order of 0.27 nm which corresponds to the (100) plane of MoS_2 nanosheets, can be observed in figure 1(b) [10]. The inset of figure 1(b) shows the SEAD pattern of MoS_2 confirming the crystallinity of the exfoliated nanosheets. Raman spectra in figure 1(c) show the peak difference of ~25 cm^{-1} between the characteristic peaks of MoS_2 confirming the presence of a few layers [23]. Also, the photoluminescence spectra of MoS_2 layers shown in figure 1(d) reveal that the band gap value of synthesized MoS_2 nanosheets is around 1.75 eV.

Figures 2(a) and (b) shows SEM image of exfoliated nanosheets and the corresponding lateral area distribution of the flakes respectively. The average flake area is found to be 0.4663 μm^2. Figure 2(c) shows the EDS spectra of MoS_2 nanosheets and the spectra confirm that the as-synthesized MoS_2 nanostructures contain Mo and S elements along with oxygen. The AFM image of MoS_2 nanosheets is shown in figure 2(d). The average roughness (Ra) and root mean square roughness (R_q) of MoS_2 layers is 1.2 nm and 3.1 nm respectively. The thickness distribution of exfoliated nanosheets, analyzed using AFM is shown in figure 2 (e). The average flake thickness is around 2.96 nm. This suggested that bulk MoS_2 particles are successfully exfoliated and significantly fragmented.

To quantify the piezoelectric response at the nanoscale, the PFM based investigations were carried out using AFM in contact mode. For local piezoelectric study, common AFM provides an ideal platform, due to high vertical resolution and high localization of electric field at the junction between the metalized tip and the surface. The PFM uses the basic principle of inverse piezoelectric effect wherein AC field is applied onto the sample surface through AFM probe keeping the bottom electrode grounded, which results in the surface deformation of the sample. The amplitude/phase of this precise deformation could be measured to characterize the strength/direction of the dipole. The tip-sample voltage is adjusted with a periodic tip bias

$$V_{tip} = V_{DC} + V_{AC}\cos(\omega t) \quad (1)$$

here the drive frequency ω is chosen to be well above the feedback bandwidth. This drive is responsible for generating an oscillating electric field below the tip that can induce localized deformation in the MoS_2 surface.

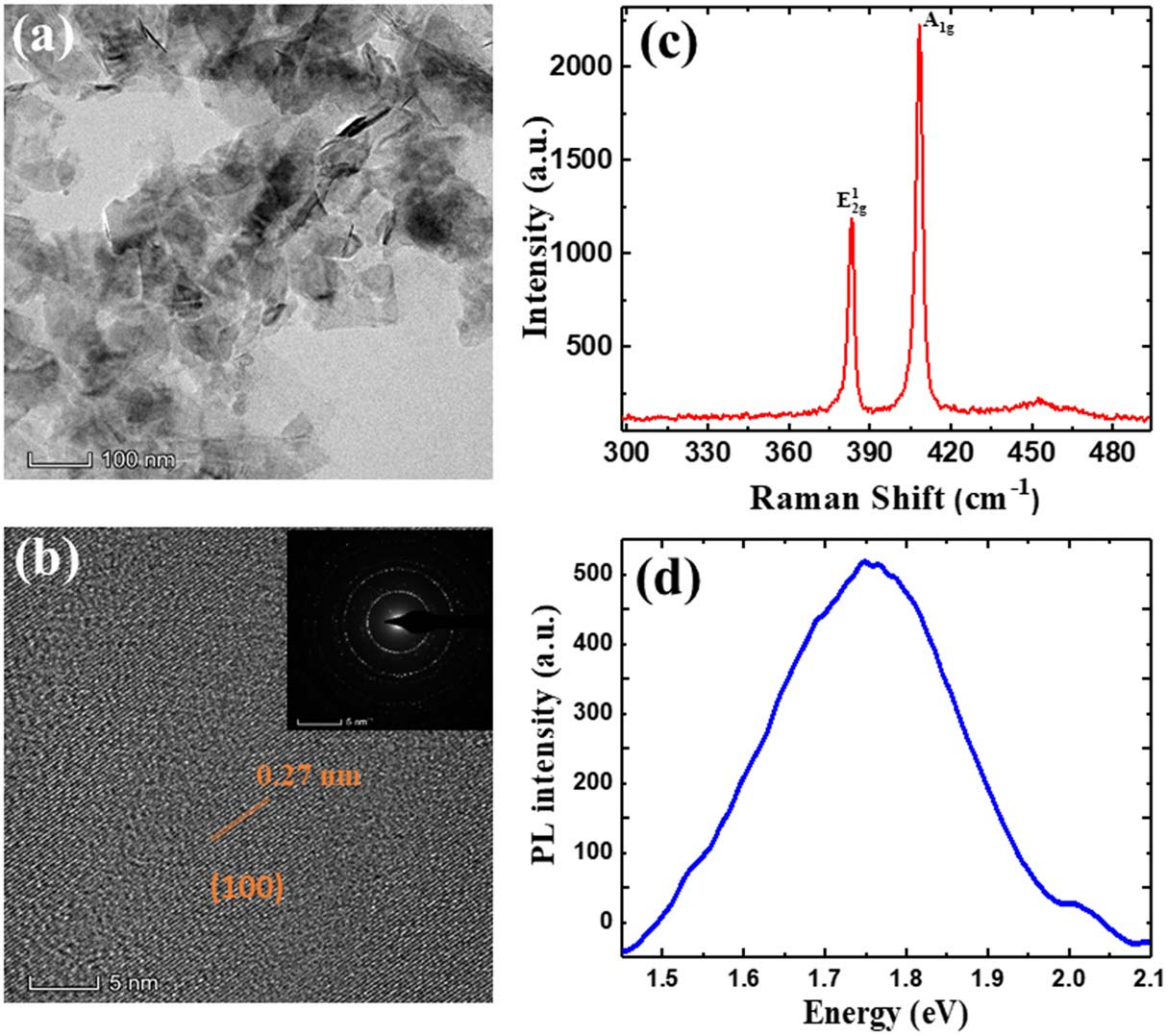

Figure 1. (a) TEM and (b) HRTEM images with inset 1 (b) showing the SAED pattern of MoS_2 nanosheets. (c) Raman spectra and (d) photoluminescence spectra of a few layers of MoS_2.

During the measurement, the cantilever oscillation frequency was directed close to its resonant frequency with $V_{bias} = 6$ V. The drive frequency of 50 kHz was chosen to optimize the signal stability and signal-to-noise ratio, as there was less than 20% variation in PFM amplitude signal in the frequency range of 20–60 kHz.

The PFM measurements were carried out on a few layers of MoS_2, where the nanosheets were not agglomerated. Throughout the PFM measurements, the cantilever tip (Bruker SCM-PIT) of AFM acts as a top electrode and ITO coated substrate as the bottom electrode. Figures 3(a)–(c) shows the topography, amplitude, and phase image of typical MoS_2 layers deposited on to ITO substrate. The deflection sensitivity of the system (48 V μm^{-1}) was determined using force-distance (F-D) curve (figure 3(d)) by indenting the cantilever tip on a hard surface of sapphire. To get electrostatic free piezoresponse, the voltage was applied during PFM measurements and a stiffer (2.945 N m^{-1}) cantilever was used throughout the measurement. The comparison of the input voltage with periodic surface vibrations using a lock-in amplifier was used to quantify the PFM response in terms of its amplitude (A) and phase (φ) signals. The characteristic butterfly loop in the PFM amplitude and the hysteresis loop in the phase signal as a function of applied voltage for a few layers of MoS_2 are also shown in figures 3(e) and (f) respectively. To determine the value of the piezoelectric constant, the piezoresponse was measured by different driving voltages repeatedly. The change in PFM amplitude indicates mechanical responses with respect to the electrical signal of V_{tip} confirming the piezoelectric effect from MoS_2 nanosheets. To quantify the effect, the linear piezoelectricity can be determined by the following equation [24]

$$A = d_{33} V_{AC}, \tag{2}$$

where A is the PFM amplitude, V_{AC} is the drive ac bias voltage and d_{33} is the effective piezoelectric coefficient. The measurements were conducted in the strong-indentation regime, where the piezo-response is dominated by the d_{33} rather than d_{31} of the material. Here d_{33} is the induced strain in direction 3 per unit electric field applied in direction 3 whereas d_{31} is the induced strain in direction 1 per unit electric field applied in direction 3. From the plot of piezo-response amplitude versus V_{bias}, taken on the MoS_2 layers

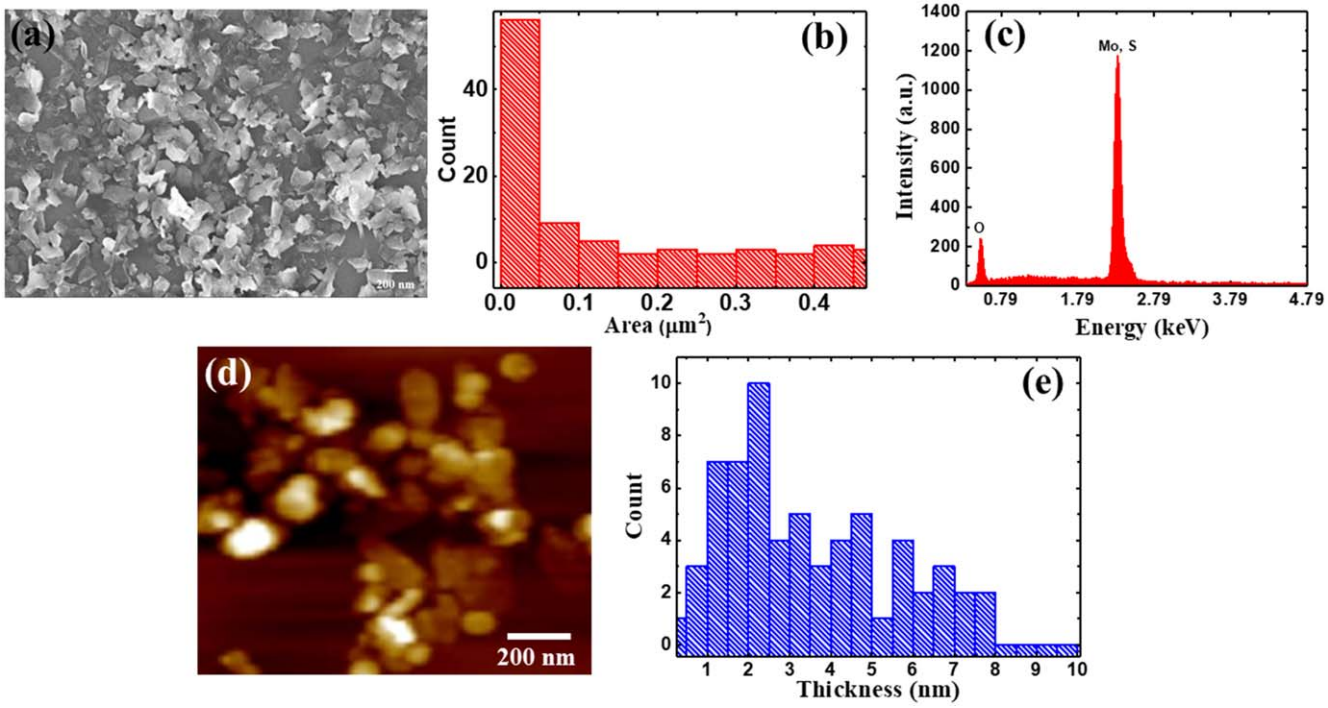

Figure 2. Nanosheet distribution is shown by SEM and AFM images. (a) SEM image of nanosheets (b) nanosheets lateral area distribution of nanosheets, (c) EDS spectra (d) AFM image of nanosheets, and (e) thickness distribution of MoS_2 nanosheets.

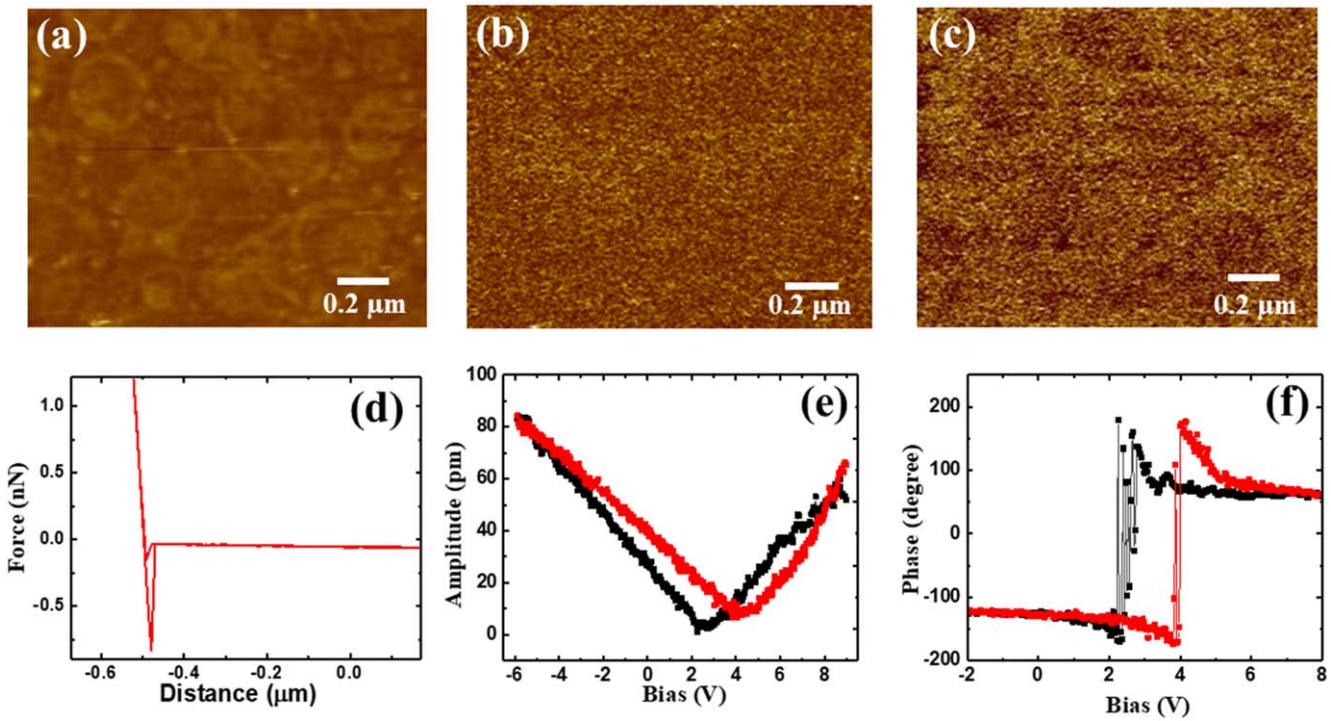

Figure 3. PFM measurements on MoS_2 nanosheets, (a) topography image (b) corresponding amplitude signal, and (c) PFM phase image of few layer MoS_2 nanosheets. Typical measurements made during the PFM measurement include (d) force distance curve measured from the clean standard sapphire surface, (e) PFM amplitude and (f) PFM phase hysteresis loop measured from (b) and (c) are shown.

(figure 3(e)), we extracted the effective piezoelectric coefficient value (d_{33}) to be 9.6 pm V^{-1}.

Due to the small-scale effect, the classical piezoelectricity caused by the non-centrosymmetric crystal structure will not be dominant in our case [25]. To confirm that this response was not coming only because of the classical piezoelectricity of MoS_2 in odd number of layers, the piezo response of MoS_2 having different thicknesses (monolayer, bilayer, and trilayer) was investigated by PFM under similar imaging parameters. All the PFM measurements were carried out in the

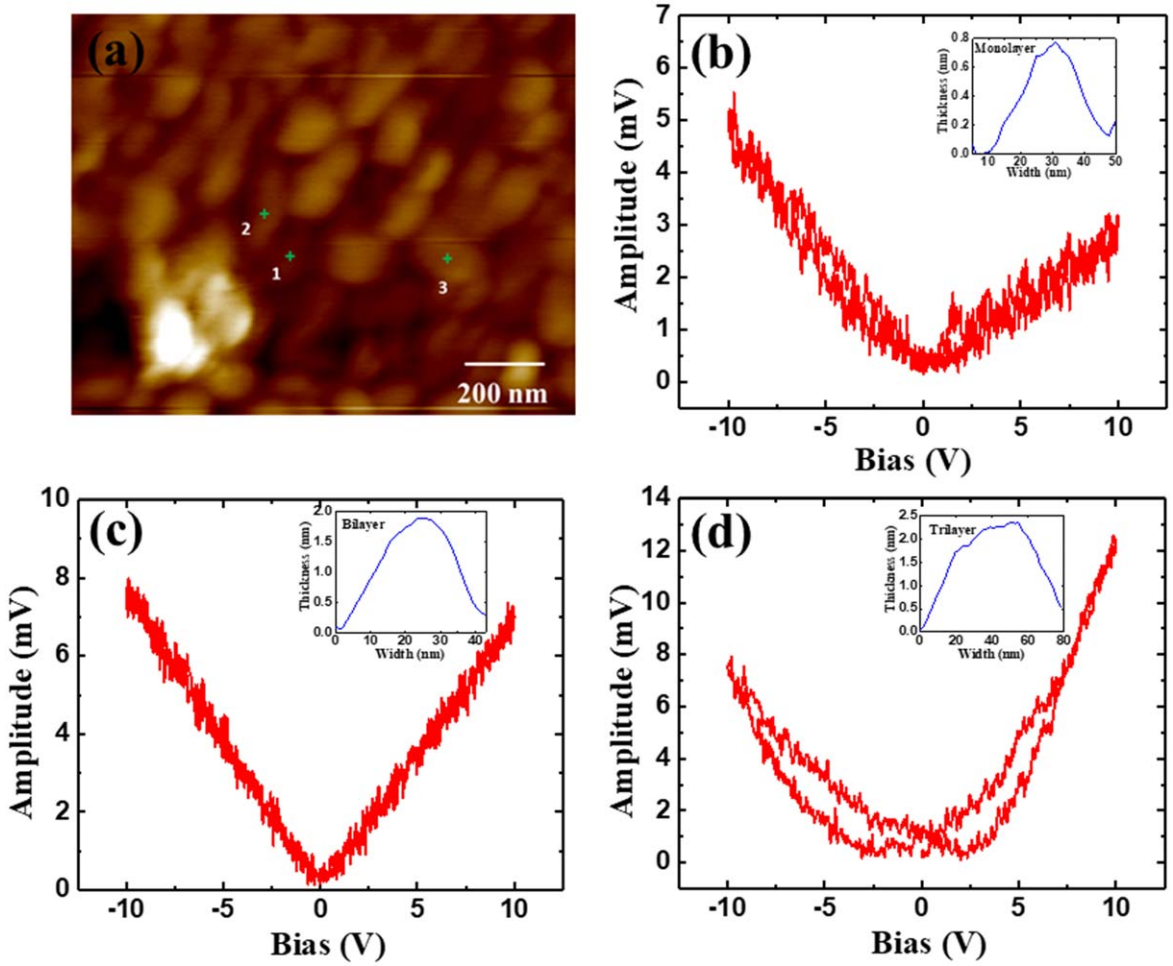

Figure 4. (a) Topographic AFM image showing monolayer (1), bilayer (2), and trilayer. (3) MoS_2. The PFM amplitude of (b) monolayer (c) bilayer and (d) trilayer MoS_2. The inset shows the respective thickness plots of the MoS_2 nanosheets from the topographic image shown in figure 4(a) on which the PFM measurements were made.

ramping voltage range of −10 V to +10 V for MoS_2 having a different thicknesses as shown in figure 4. The AFM topography of the MoS_2 sample, consisting of mono, bi, and tri-layer of MoS_2 is marked as 1, 2, and 3 respectively in figure 4(a). The PFM amplitude signal as a function of ramped Vbias at the frequency of 50 kHz for respective mono-, bi- and tri-layer of MoS_2 are shown in figures 4(b)–(d). Different AC voltages were applied from the AFM tip to calculate the piezoelectric coefficient, which reveals a linear relationship between the applied electric field and mechanical deformation. As expected, a strong piezoelectric response was observed from monolayer MoS_2. From the piezo-response amplitude versus V_{bias} curves taken on the spots marked by the plus signs (figure 4(a)), we extracted the effective piezoelectric coefficient (d_{33}) value of 10.91 pm V^{-1}, 15.75 pm $V^{-1,}$ and 25.14 pm V^{-1} for monolayer, bilayer, and tri-layer respectively. The decrease in d_{33} value in the case of a few layers may be due to the screening effect induced by free carriers. The material with a higher piezoelectric coefficient produces more electricity for a given strain thus improving the efficiency of the piezoelectric device.

In general, the piezoelectric effect appears when external mechanical stress breaks the atomic symmetry of a material, which causes the accumulation of electric charges. In the case of even layered MoS_2, the piezoelectricity from alternating layers is canceled out. Therefore, the piezo response has been observed in odd number of layers of MoS_2 [9]. The piezoelectric response from MoS_2 in this work is probably coming because of defects as observed through EDS analysis. There is a possibility of trapping and stabilization of charges around the defects in the material as reported by A. Apte *et al* [26] that can induce a piezoelectric response. The synthesis procedure in this work gives rise to oxidation which suggests an efficient route to artificially engineer piezoelectricity in TMDC.

To further verify the presence of defects, XPS measurements have been performed. In the full survey spectra shown in figure 5(a), the characteristic peaks of Mo, S, O, and Si (due to substrate) atoms were observed. In the image, except for C1s peak, no other impurity peak can be found. The corresponding binding energy plots for Mo 3d, S 2p, and O 1s are presented in figures 5(b)–(d) respectively. All spectra were referenced by adventitious carbon 1S peak at 284.8 eV (not shown). In the Mo 3d spectra of as-prepared MoS_2 layers, the characteristic peaks at 229.25 eV and 231.41 eV

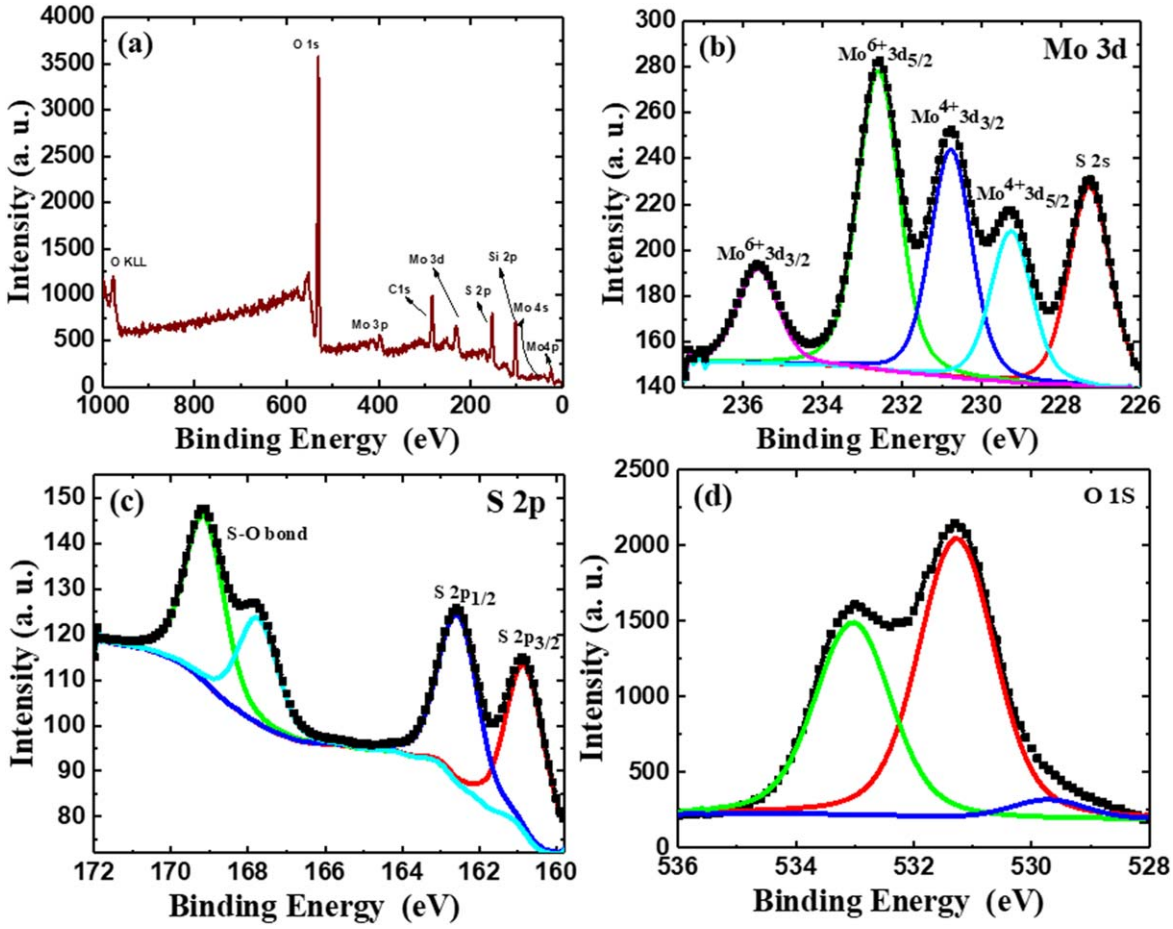

Figure 5. XPS spectra of MoS_2 surface (a) full survey spectrum. The high-resolution scanning of the (b) Mo 3d (c) S 2p and (d) O 1s peaks.

belong to the Mo^{4+} $3d_{5/2}$ and Mo^{4+} $3d_{3/2}$ components of MoS_2, respectively [27, 28].

The peak at 227.27 eV arises due to S 2s component of MoS_2 [27]. The binding energies of Mo 3d and S 2p regions reveal that the few layer MoS_2 has a strong trigonal prismatic structure. The peak at binding energies 232.59 eV and 235.6 eV are ascribed to Mo^{6+} revealing that the Mo edges in MoS_2 layers are slightly oxidized during the transition from the Mo^{4+} state to the Mo^{6+} state which corresponds to the Mo(VI) species (Mo^{6+} $3d_{5/2}$ and Mo^{6+} $3d_{3/2}$) in MoO_x [29, 30]. Therefore, peaks attribute to the formation of Mo–O suggesting some degree of MoO_x-like structures. Here in MoS_2, oxygen can be attached as substitutional atoms at sulfur sites or as atoms bound to Mo atoms at plane edges. Additionally, there are two strong peaks at 162.07 eV and 163.3 eV which are assigned to S $2p_{3/2}$ and S $2p_{3/2}$ binding energies for S^{2-}. The peak at 169.2 eV could be ascribed to the existence of an S–O bond[29] which indicates partial oxidation of the S edges in MoS_2 layers. The oxidation percentage of Mo and S edges was 12.04% and 27.13% respectively. The charges and dipoles are trapped at the defect sites of MoS_2 flakes. These induced defects act as nucleation and pinning centers for moving domain walls. It has been observed earlier that the motion of the domain wall is a significant contributor to the piezoelectric coefficient [31]. Hence, we believe, the defects induced in MoS_2 flakes during the synthesis process result into the piezoelectric response in the few layers of MoS_2.

5. Summary

In summary, a strong piezoelectric response in modified liquid exfoliated MoS_2 nanosheets has been observed. The strong piezoelectric coefficient in MoS_2 is attributed to the formation of defects during its synthesis process which is confirmed by XPS analysis. The defects promote the creation of a local asymmetric structure which gives rise to strong piezo-response. This work suggests an efficient route to artificially engineer piezoelectricity in MoS_2. Given the material's properties and piezoelectric response, the liquid exfoliated MoS_2 could be considered a promising candidate for piezotronics devices and energy harvesting technology.

Acknowledgments

Authors are thankful to CeNSE, IISc Bangalore for TEM, SEM, AFM, Raman, XPS, and PFM measurements. JS would like to thank SERB, India for NPDF fellowship.

Data availability statement

The data that support the findings of this study are available upon reasonable request from the authors.

ORCID iDs

Jyoti Shakya https://orcid.org/0000-0001-6403-2755
Gayathri H N https://orcid.org/0000-0002-0844-1164

References

[1] Cash D W 2018 Choices on the road to the clean energy future *Energy Res. Soc. Sci.* **35** 224–6
[2] Dincer I and Acar C 2015 A review on clean energy solutions for better sustainability *Int. J. Energy Res.* **39** 585–606
[3] Shin D M, Hong S W and Hwang Y H 2020 Recent advances in organic piezoelectric biomaterials for energy and biomedical applications *Nanomaterials* **10** 123
[4] Sharma N D, Maranganti R and Sharma P 2007 On the possibility of piezoelectric nanocomposites without using piezoelectric materials *J. Mech. Phys. Solids* **55** 2328–50
[5] Swallow L M, Luo J K, Siores E, Patel I and Dodds D 2008 A piezoelectric fibre composite based energy harvesting device for potential wearable applications *Smart Mater. Struct.* **17** 025017
[6] Cui C, Xue F, Hu W J and Li L J 2018 Two-dimensional materials with piezoelectric and ferroelectric functionalities *npj 2D Mater. Appl.* **2** 1–14
[7] Song X, Hui F, Knobloch T, Wang B, Fan Z, Grasser T, Jing X, Shi Y and Lanza M 2017 Piezoelectricity in two dimensions: graphene versus molybdenum disulfide *Appl. Phys. Lett.* **111** 083107
[8] Rostami H, Guinea F, Polini M and Roldán R 2018 Piezoelectricity and valley chern number in inhomogeneous hexagonal 2D crystals *npj 2D Mater. Appl.* **2** 1–6
[9] Wu W *et al* 2014 Piezoelectricity of single-atomic-layer MoS_2 for energy conversion and piezotronics *Nature* **514** 470–4
[10] Peng Y, Que M, Tao J, Wang X, Lu J, Hu G, Wan B, Xu Q and Pan C 2018 Progress in piezotronic and piezo-phototronic effect of 2D materials *2D Mater.* **5** 042003
[11] Duerloo K N, Ong M T and Reed E J 2012 Intrinsic piezoelectricity in two-dimensional materials *J. Phys. Chem. Lett.* **3** 2871
[12] Ebnonnasir A, Narayanan B, Kodambaka S and Ciobanu C V 2014 Tunable MoS_2 bandgap in MoS_2-graphene heterostructures *Appl. Phys. Lett.* **105** 031603
[13] Shakya J, Patel A S, Singh F and Mohanty T 2016 Composition dependent Fermi level shifting of Au decorated MoS_2 nanosheets *Appl. Phys. Lett.* **108** 013103
[14] Huo N, Yang Y, Wu Y N, Zhang X G, Pantelidese S T and Konstantatos G 2018 High carrier mobility in monolayer CVD-grown MoS_2 through phonon suppression *Nanoscale* **10** 15071–7
[15] Li T and Galli G 2007 Electronic properties of MoS_2 nanoparticles *J. Phys. Chem.* C **111** 16192–6
[16] Shakya J, Kumar S, Kanjilal D and Mohanty T 2017 Work function modulation of molybdenum disulfide nanosheets by introducing systematic lattice strain *Sci. Rep.* **7** 9576
[17] Muralikrishna S, Manjunath K, Samrat D, Reddy V, Ramakrishnappa T and Nagaraju D H 2015 Hydrothermal synthesis of 2D MoS_2 nanosheets for electrocatalytic hydrogen evolution reaction *RSC Adv.* **5** 89389
[18] Bergeron H, Sangwan V K, McMorrow J J, Campbel G P, Balla I, Liu X, Bedzyk M J, Marks T J and Hersam M C 2017 Chemical vapor deposition of monolayer MoS_2 directly on ultrathin Al_2O_3 for low-power electronics *Appl. Phys. Lett.* **110** 053101
[19] Ma H, Shen Z and Ben S 2018 Understanding the exfoliation and dispersion of MoS_2 nanosheets in pure water *J. Colloid Interface Sci.* **517** 204–12
[20] Li H, Wu J, Yin Z and Zhang H 2014 Preparation and applications of mechanically exfoliated single-layer and multilayer MoS_2 and WSe_2 nanosheets *Acc. Chem. Res.* **47** 1067–75
[21] Jin H J, Yoon W Y and Jo W 2018 Virtual out-of-plane piezoelectric response in MoS_2 layers controlled by ferroelectric polarization *ACS Appl. Mater. Interfaces* **10** 1334–9
[22] Michel K H and Verberck B 2011 Phonon dispersions and piezoelectricity in bulk and multilayers of hexagonal boron nitride *Phys. Rev.* B **83** 115328
[23] Lee C, Yan H, Brus L E, Heinz T F, Hone J and Ryu S 2010 Anomalous lattice vibrations of single-and few-layer MoS_2 *ACS Nano* **4** 2695–700
[24] Brennan C J, Ghosh R, Koul K, Banerjee S K, Lu N and Yu E T 2017 Out-of-plane electromechanical response of monolayer molybdenum disulfide measured by piezoresponse force microscopy *Nano Lett.* **17** 5464–71
[25] Huang Y, Li L, Sha J and Chen Y 2017 Size-dependent piezoelectricity of molybdenum disulfide (MoS_2) films obtained by atomic layer deposition (ALD) *Appl. Phys. Lett.* **111** 063902
[26] Apte A *et al* 2020 2D electrets of ultrathin MoO_2 with apparent piezoelectricity *Adv. Mater.* **32** 2000006
[27] Adilbekova B, Lin Y, Yengel E, Faber H, Harrison G, Firdaus Y, El-Labban A, Anjum D H, Tung V and Anthopoulos T D 2020 Liquid phase exfoliation of MoS_2 and WS_2 in aqueous ammonia and their application in highly efficient organic solar cells *J. Mater. Chem.* C **8** 5259
[28] Wang Y, He Z, Zhang J, Liu H, Lai X, Liu B, Chen Y, Wang F and Zhang L 2020 UV illumination enhanced desorption of oxygen molecules from monolayer MoS_2 surface *Nano Res.* **13** 358–65
[29] Ghasemi F and Mohajerzadeh S 2016 Sequential solvent exchange method for controlled exfoliation of MoS_2 suitable for phototransistor fabrication *ACS Appl. Mater. Interfaces* **8** 31179–91
[30] Hussain S *et al* 2016 Large-area, continuous and high electrical performances of bilayer to few layers MoS_2 fabricated by RF sputtering via post-deposition annealing method *Sci. Rep.* **6** 1–13
[31] Gharb N B, Fujii I, Hong E, McKinstry S T, Taylor D V and Damjanovic D 2007 Domain wall contributions to the properties of piezoelectric thin films *J. Electroceram.* **19** 49–67